NT@UW-10-19

arXiv:1008.4345v3 [hep-ph] 9 Sep 2010

Third Zemach Moment of the Proton

Ian C. Cloët[1] and Gerald A. Miller[1]

[1]*Department of Physics, University of Washington, Seattle, WA 98195-1560*

Modern electron scattering experiments have determined the proton electric form factor, $G_{Ep}(Q^2)$, to high precision. We utilize this data, represented by the different empirical form factor parametrizations, to compute the third Zemach moment of the proton charge distribution. We find that existing data rule out a value of the third Zemach moment large enough to explain the current puzzle with the proton charge radius, determined from the Lamb shift in muonic hydrogen. This is in contrast with the recent paper of De Rújula. We also demonstrate that the size of the third Zemach moment is largely governed by the fourth moment of the conventional charge distributions, $\langle r^4 \rangle$, which enables us to obtain a rigorous upper bound on the magnitude of the proton's third Zemach moment.

PACS numbers: 36.10.Ee, 31.30.jr, 13.40.Em, 13.40.Gp
Keywords: form factor, proton charge density, proton radius

Pohl *et al.* recently reported a very precise measurement of the Lamb shift in muonic hydrogen, that leads to a proton radius of [1]

$$\langle r_p^2 \rangle^{1/2} = 0.84184 \pm 0.00067\,\text{fm}, \tag{1}$$

which is five standard deviations away from the CODATA compilation of [2]

$$\langle r_p^2 \rangle^{1/2} = 0.8768 \pm 0.0069\,\text{fm}. \tag{2}$$

There has been much speculation about the origin and possible consequences of the puzzling difference between the results of muonic and electronic hydrogen.

Even more recently De Rújula [3] pointed out that the discrepancy between the two results can be removed if the proton's third Zemach moment is very large. He finds that a value of

$$\langle r_p^3 \rangle_{(2)} = 36.6 \pm 6.9\,\text{fm}^3, \tag{3}$$

combines the impressive experimental results from the CODATA compilation and the recent muonic Lamb shift data in a consistent manner. This result is more than 13 times larger than the experimental extraction of Friar and Sick [4], who use electron-proton scattering data to determine

$$\langle r_p^3 \rangle_{(2)} = 2.71 \pm 0.13\,\text{fm}^3. \tag{4}$$

It is noteworthy that the length scale associated with Eq. (3) is about four times the proton root-mean-square radius. Such a large value is supported in Ref. [3] by a "toy model" of the proton electric form factor, namely

$$G_E^{\text{De Rújula}}(Q^2) = \frac{1}{D}\left[\frac{c^2\,M^4}{Q^2+M^2} + \frac{s^2\,m^6}{\left(Q^2+m^2\right)^2}\right], \tag{5}$$

where $s^2 \equiv \sin^2\theta$, $c^2 \equiv \cos^2\theta$ and $D \equiv c^2\,M^2 + s^2\,m^2$. The CODATA charge radius result and the large Zemach moment of Eq. (3) can be accommodated for a range of mass parameters and mixing angle. For $s^2 = 0.3$ the mass scales are typically $m \simeq 15\,\text{MeV}$ and $M \simeq 750\,\text{MeV}$ [3]. For these parameters we have plotted Eq. (5) as the dotted line in Fig. 1, where it is compared with a dipole form factor and the empirical parameterizations from Refs. [5, 6]. The severe disagreement between the form factor of Eq. (5) and the realistic form factors of Refs. [5, 6] demonstrate that this "toy model" is not a viable representation of the data.

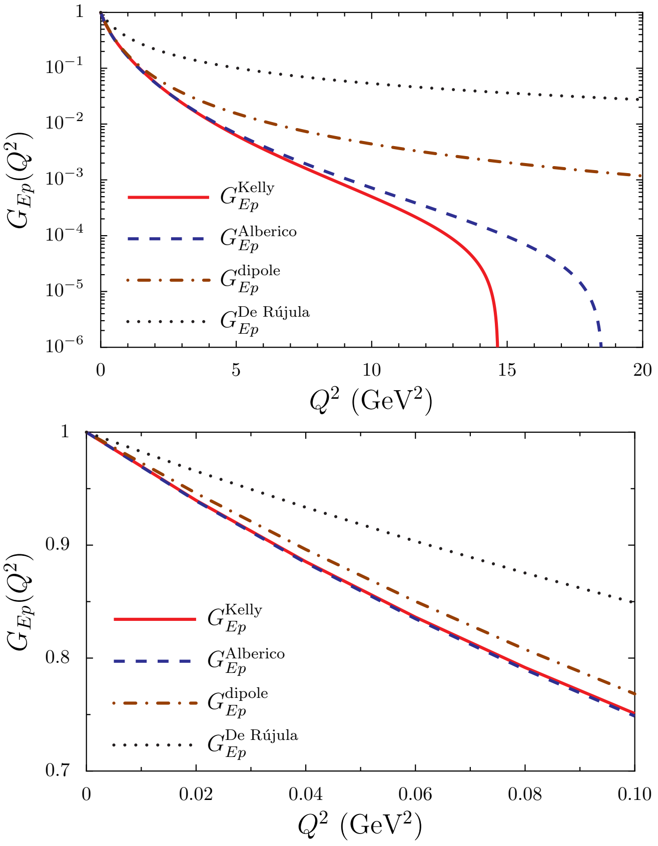

FIG. 1: The proton G_{Ep} form factor from the parameterizations of Kelly [5] (solid line), fit II from Alberico *et al.* [6] (dashed line) and the dipole form factor of Eq. (6) is given as the dot-dashed line. The "toy model" of Ref. [3], with $\sin^2\theta = 0.3$, $m = 15\,\text{MeV}$ and $M = 750\,\text{MeV}$, is illustrated as the dotted line.

parameterization	$\langle r_p^3\rangle_{(2)}$ [fm^3]	$\langle r_p^2\rangle$ [fm^2]	$\langle r_p^2\rangle^{1/2}$ [fm]	$\langle r_p^4\rangle$ [fm^4]	$\langle r_p^3\rangle_{(2)}^{\text{max}}$ [fm^3]
Dipole (Eq. (6))	2.023	0.658	0.811	1.083	3.029
Kelly [5]	2.524	0.744	0.863	1.619	4.067
Alberico *et al.* [6]	2.545	0.750	0.866	1.623	4.097

TABLE I: Values of the third Zemach moment $\langle r_p^3\rangle_{(2)}$, the mean-square charge radius $\langle r_p^2\rangle$, the charge radius $\langle r_p^2\rangle^{1/2}$ and the fourth moment of the charge distribution $\langle r_p^4\rangle$, for each of the three proton form factor parameterizations considered. The last column containing $\langle r_p^3\rangle_{(2)}^{\text{max}}$ represents the upper bound on the third Zemach moment of the proton given by Eq. (15), with $\mu = 1\,\text{GeV}$.

Nevertheless, it is reasonable to ask if the use of a realistic extraction of G_{Ep} leads to a value of the Zemach radius very different from that obtained from the typically used dipole form, namely

$$G_E^{\text{dipole}}(Q^2) = \left(1 + \frac{Q^2}{\Lambda^2}\right)^{-2}, \tag{6}$$

where $\Lambda^2 = 0.71\,\text{GeV}^2$. This form has historical validity in describing early data and was explicitly assumed in the recent experimental analysis of Pohl *et al.* [1]. However, several experiments (see for example the review of Ref. [7]) have found that G_{Ep} actually falls faster than the dipole. Therefore, we use two different more recent parametrizations from Refs. [5, 6]. These parametrizations take the general form

$$G_E(Q^2) = \frac{1 + \sum_{n=1}^{N} a_n \tau^n}{1 + \sum_{n=1}^{N} b_n \tau^n}, \quad \text{where} \quad \tau \equiv \frac{Q^2}{4\,m_p^2}, \tag{7}$$

with proton mass labeled by m_p and the various coefficients are given in Refs. [5, 6]. Note, we use fit II for the Alberico *et al.* [6] parameterization. These empirical results for the proton G_{Ep} form factor are illustrated in Fig. 1.

The third Zemach moment is defined by

$$\langle r_p^3\rangle_{(2)} \equiv \int d^3r\; r^3 \rho_2(r), \tag{8}$$

where

$$\begin{aligned} \rho_2(r) &= \int d^3r' \rho_p(\mathbf{r}')\rho_p(|\mathbf{r}' - \mathbf{r}|), \\ &= \int \frac{d^3q}{(2\pi)^3}\, e^{-i\,\mathbf{q}\cdot\mathbf{r}}\, G_E^2(\mathbf{q}^2). \end{aligned} \tag{9}$$

The conventional proton charge density, $\rho_p(r)$, is defined by

$$\rho_p(r) \equiv \int \frac{d^3q}{(2\pi)^3} e^{-i\,\mathbf{q}\cdot\mathbf{r}}\, G_{Ep}(\mathbf{q}^2), \tag{10}$$

with the charge radius given by

$$\langle r_p^2\rangle = \int d^3r\; r^2 \rho_p(r). \tag{11}$$

The results of our numerical evaluations are presented in Table I. Observe that the values of $\langle r_p^3\rangle_{(2)}$ are smaller than that of Eq. (3) by approximately a factor of 15. However, the agreement with the empirical result of Ref. [4] (see Eq. (4)) is fairly good. The G_{Ep} parameterizations of Refs. [5, 6] fall faster with increasing Q^2 than the dipole form factor (see Fig. 1), leading to coordinate space distributions of greater extent. Therefore, the values of the third Zemach moment $\langle r_p^3\rangle_{(2)}$ and the mean-square radius $\langle r_p^2\rangle$ both increase relative to the values obtained from the dipole form factor.

Examination of the integrand in Eq. (8) for each of the three form factor models, reveals that 80% of the strength for the Zemach moment comes from the domain where Q^2 is less than $1\,\text{GeV}^2$ and 50% from Q^2 values less than $0.25\,\text{GeV}^2$. Therefore, the quoted values of the Zemach moment given in Table I are insensitive to the model dependent extrapolation to infinite Q^2. In the experimental extraction of the charge radius by Pohl *et al.* [1], the third Zemach moment is suppressed relative to the charge radius by a factor of ~ 570, therefore the variation of the Zemach moment observed in Table I has negligible impact on the extracted value of the charge radius.

It is possible to obtain a rigorous upper bound on the third Zemach moment of the proton using the result [4]

$$\langle r_p^3\rangle_{(2)} = \frac{48}{\pi}\int_0^\infty \frac{dq}{q^4}\left[G_{Ep}(q^2)^2 + \frac{q^2}{3}\langle r_p^2\rangle - 1\right]. \tag{12}$$

The integrand in Eq. (12) is a monotonically decreasing positive definite function on the integration domain, with a maximum at $q = 0$ given by

$$I(q = 0) = \frac{48}{\pi}\left[\frac{1}{60}\langle r_p^4\rangle + \frac{1}{36}\langle r_p^2\rangle^2\right]. \tag{13}$$

For moderate to large q the integrand in Eq. (12) is completely saturated by the last two terms, that is

$$I \to \frac{48}{\pi}\frac{1}{q^4}\left[\frac{q^2}{3}\langle r_p^2\rangle - 1\right]. \tag{14}$$

Empirically we know that at $q = 1\,\text{GeV}$ the above expression represents $\sim 99.5\%$ of the integrand in Eq. (12). This is illustrated in Fig. 2 for the dipole form factor of Eq. (6), where we plot the integrand of Eq. (12) and Eq. (14). The integrand of Eq. (12) coincides with Eq. (14)

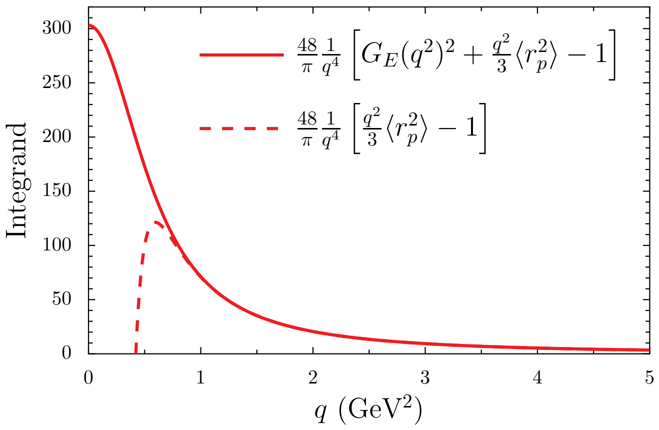

FIG. 2: Plot of the integrand in Eq. (12) (solid line) and the dominate piece at moderate to large q given by Eq. (14) (dashed line).

for $q \gtrsim 1\,$GeV, this is also the case for the empirical form factors of Refs. [5, 6] and the model of De Rujula.

Therefore, the third Zemach moment has a rigorous upper bound given by

$$\langle r_p^3\rangle_{(2)} \leqslant \frac{4}{5\,\pi}\left[\langle r_p^4\rangle+\frac{5}{3}\,\langle r_p^2\rangle^2\right]\mu+\frac{16}{\pi\,\mu}\left[\langle r_p^2\rangle+\frac{1}{\mu^2}\right]. \tag{15}$$

where the first term is the area of the rectangle defined by the integrand upper bound of Eq. (13) and $0 \leqslant q \leqslant \mu\,$GeV, whereas the second term results from integrating Eq. (14) from $q = \mu\,$GeV to infinity. For the reasons discussed above we expect that $\mu = 1\,$GeV is a conservative choice for the evaluation of the upper bound given in Eq. (15). It is therefore apparent that if a model reproduces the proton charge radius, a large third Zemach moment can only occur if $\langle r_p^4\rangle$ is also large. Typical empirical values are given in the second last column of Table I, whereas the model of De Rujula, expressed in Eq. (5), gives $\langle r_p^4\rangle = 1849\,\mathrm{fm}^4$. The upper bound for the third Zemach moment of the proton obtained from Eq. (15), with $\mu = 1\,$GeV, is given in the last column of Table I where it is labeled by $\langle r_p^3\rangle_{(2)}^{\max}$.

The net result is that the published parametrizations, which take into account a wide variety of electron scattering data, cannot account for the value of the third Zemach moment found in Ref. [3]. It is likely that further investigations of low Q^2 data will lead to improved parametrizations for G_{Ep} [8]. However, enhancing the Zemach moment significantly above the dipole result is extremely unlikely. We believe that the resolution of the current puzzle regarding the proton radius, determined from the muon and electron Lamb shifts in hydrogen, lies in a direction other than that suggested by De Rújula.

Acknowledgments

This research was supported by the United States Department of Energy. We thank R. Gilman for informing us about Ref. [3] and York Schroeder for bringing to our attention errors in the original version of Ref. [3].

---

[1] R. Pohl, A. Antognini, F. Nez *et al.*, Nature **466**, 213-216 (2010).
[2] P. J. Mohr, B. N. Taylor and D. B. Newell, Rev. Mod. Phys. **80**, 633 (2008).
[3] A. De Rujula, arXiv:1008.3861v3 [hep-ph].
[4] J. L. Friar and I. Sick, Phys. Rev. A **72**, 040502(R) (2005).
[5] J. J. Kelly, Phys. Rev. C **70**, 068202 (2004).
[6] W. M. Alberico, S. M. Bilenky, C. Giunti and K. M. Graczyk, Phys. Rev. C **79**, 065204 (2009).
[7] C. F. Perdrisat, V. Punjabi and M. Vanderhaeghen, Prog. Part. Nucl. Phys. **59**, 694 (2007).
[8] J. Arrington, private communication.